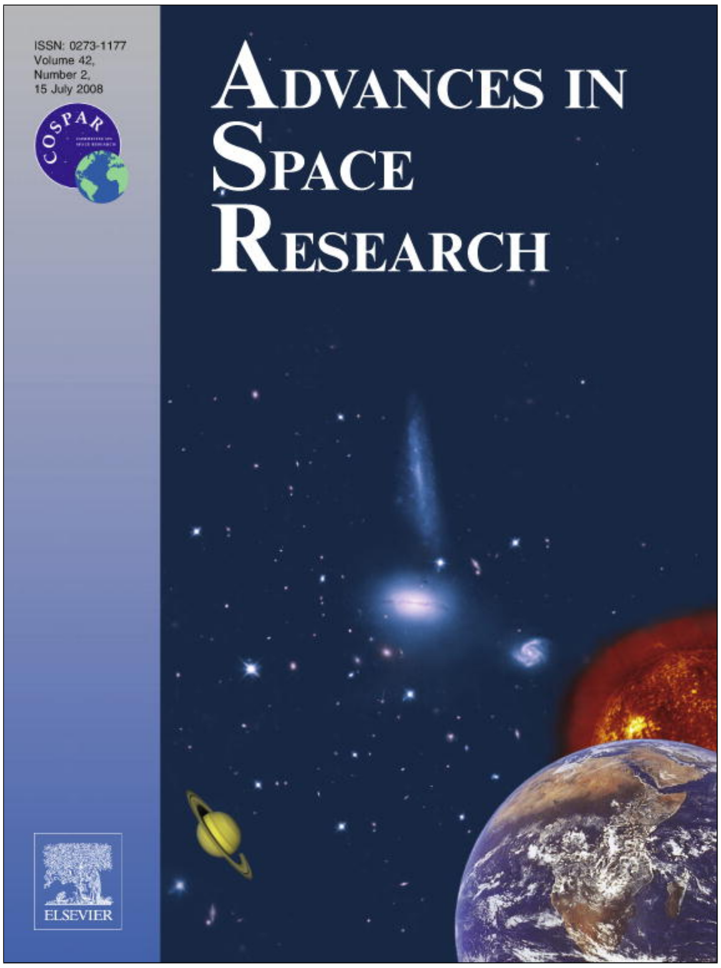
ISSN: 0273-1177
Volume 42,
Number 2,
15 July 2008
COSPAR
ADVANCES IN
SPACE
RESEARCH
ELSEVIER

Available online at www.sciencedirect.com
ScienceDirect
ELSEVIER
Advances in Space Research 42 (2008) 248–258
ADVANCES IN SPACE RESEARCH (a COSPAR publication)
www.elsevier.com/locate/asr

Lunar international science coordination/calibration targets (L-ISCT)

Carle M. Pieters [a,*], James W. Head III [a], Peter Isaacson [a], Noah Petro [a], Cassandra Runyon [b], M. Ohtake [c], B. Föing [d], M. Grande [e]

[a] *Department of Geological Sciences, Brown University, Providence, RI 02912, USA*
[b] *Department of Geology, College of Charleston, 66 George Street, Charleston, SC 29424, USA*
[c] *Planetary Science Department, JAXA, 3-1-1 Yoshinodai, Sagamihara, Kanagawa 229-8510, Japan*
[d] *ESTEC/SCI-S, postbus 299, 2200 AG Noordwijk, Netherlands*
[e] *Institute of Mathematical and Physical Sciences, University of Wales Aberystwyth, Penglais, Aberystwyth, SY23 3BZ, Wales, UK*

Received 7 November 2006; received in revised form 19 April 2007; accepted 13 May 2007

Abstract

Eight lunar areas, each ~200 km in diameter, are identified as targets for coordinated science and instrument calibration for the orbital missions soon to be flown. Instrument teams from SELENE, Chang'E, Chandrayaan-1, and LRO are encouraged to participate in a coordinated activity of early-release data that will improve calibration and validation of data across independent and diverse instruments. The targets are representative of important lunar terrains and geologic processes and thus will also provide a broad introduction to lunar science for new investigators. We briefly identify additional cross-calibration issues for instruments that produce time series data rather than maps.

Keywords: Calibration targets; L-ISCT; International lunar targets; Lunar calibration targets

1. Introduction

A new era of international lunar exploration has begun, starting with the SMART-1 spacecraft (Europe) and continuing over the next four years with data acquired from four sophisticated remote sensing missions: SELENE (Japan), Chang'E (China), Chandrayaan-1 (India), and LRO (United States). It is recognized that this combined activity at the Moon with modern sensors will provide unprecedented new information about the Moon and will dramatically improve our understanding of Earth's nearest neighbor. It is anticipated that this blooming of scientific exploration of the Moon by nations involved in space activities will seed and foster peaceful international coordination and cooperation that will benefit all.

Presented below are eight lunar International Science Coordination/Calibration Targets (L-ISCT) that are intended to (a) allow cross-calibration of diverse multinational instruments and (b) provide a focus for training young scientists about a range of lunar science issues. Five of these targets were identified and presented during the COSPAR meeting in Beijing and were discussed more thoroughly at the subsequent 8th International Conference on Exploration and Utilization of the Moon. The concept was endorsed by the international community and included in the resulting Lunar Beijing Declaration. During a November 2006 international LRO Science Working Group meeting in Hawaii, the original five targets were expanded to include additional targets in the maria, at high latitudes, and a polar region. These eight were presented and discussed at a SELENE Science Team Meeting and later at a Chandrayaan-1 Science Team meeting in early 2007. In addition, several specific lunar areas are of common interest for ''ground truth'' (all Apollo and Luna landing sites) or science (SMART-1 and LCROSS impact sites) and are additional prime targets for coordinated study.

* Corresponding author.
E-mail address: Carle_Pieters@brown.edu (C.M. Pieters).

0273-1177/$34.00 © 2008 Published by Elsevier Ltd on behalf of COSPAR.
doi:10.1016/j.asr.2007.05.038

2. Rationale and need

Each of the missions to be flown to the Moon in the next few years has its own rationale, requirements, scientific focus, and exploration goals. Consequently, each has its own complement of sophisticated instruments and mission constraints. An overview of these missions is summarized in Table 1. Discussion of the missions and the specific instruments continues as they are implemented. Recent overviews of the missions and instruments were presented by Chin et al. (2006), Föing et al. (2006), Goswami et al. (2006), Hao and Zhou (2006), and Takizawa et al. (2006).

The surface of the Moon encompasses 38 million square kilometers and each of the polar orbiting missions in Table 1 has global access to enormously diverse lunar terrain. The processes involved to produce a calibrated global data set that is useful for comparisons with data from other instruments are both lengthy and labor intensive for each instrument. There is nevertheless great benefit to be gained from coordinating measurements between instruments of these contemporaneous orbital missions and from exchanging data early during the calibration process when possible. Although the specific calibration steps are unique to each instrument, there is much commonality across data products of different missions. A common, but limited, set of calibration targets will allow cross validation of instruments with independent information. Validation checks for similar instruments should be straightforward since the lunar surface does not change over the time scale of orbital measurements. Optical data can be compared with optical data, gamma-ray data with gamma-ray data, laser altimeter data with other topographic data, etc. It should be noted that data comparisons across different types of instruments are also highly valuable as well. For example, compositional data obtained with optical instruments should be consistent with compositional data obtained with gamma-ray and X-ray instruments, and so forth.

The eight L-ISCT targets recommended below were selected to meet several criteria. All are approximately 200 × 200 km in dimension to allow instruments with different spatial footprints to be cross-compared within a common region. A few targets are relatively homogeneous, while others exhibit (and test) diversity of coordinated measurements (topography, morphology, composition, etc.). Since the field of view varies greatly between instruments, we recommend that instruments with a small footprint target as close to the central portion as is feasible. The general locations of the eight L-ISCT areas are shown on a Clementine global albedo image of the Moon in Fig. 1 and their center coordinates are provided in Table 2.

Of equal importance to their calibration function, these areas were selected so that new or young investigators studying the Moon will learn much about the principal scientific issues concerning the Moon by calibrating and analyzing multiple data sets from these specific targets regions. As a whole, the small group of targets provides a good introduction to lunar science. The process of understanding the character of these few areas is intended to educate and spark a desire to explore further with the more extensive data produced by the various missions. These few targets provide a common starting point for much discussion and comparison among the science community and for the public to become reintroduced to the mysteries and excitement of lunar exploration. These L-ISCT areas should not be considered to be the most important science targets on the Moon; many other areas could have been selected just as easily. Instead, these targets were selected to be representative of the important science issues that orbital data can and will address. One target, Tycho crater, was explicitly chosen because of its additional outreach potential since it can be easily recognized by anyone in the world with a pair of binoculars (or exceptional eyes) and is an excellent example of a fundamental process (impact cratering) whose effect can be observed everywhere on the Moon.

Each of the L-ISCT are identified and briefly described below. In preparation for a successful international venture with coordinated data, the first step over the next year is compilation of current data for these L-ISCT sites. The most productive steps will occur over the next several years

Table 1
International Lunar Missions (details presented by Föing et al., 2006; Takizawa et al., 2006, Hao and Zhou, 2006, Goswami et al., 2006, and Chin et al., 2006)

	SMART-1 [ESA]	SELENE [JAXA]	Chang'E [CNSA]	Chandrayaan-1 [ISRO]	LRO [NASA]
Launch	2003	2007	2007/8	2008	2008
Orbit	400 × 4000 km polar	100 km polar circular	200 km polar circular	100 km polar circular	50 km polar circular
Objectives	Technology demonstration; instrument tests, September 2006 impact ending	Lunar origin and evolution; develop technology for future lunar exploration	Surface structure, topography, composition; particle environment	Integrated composition and terrain mapping science; demonstrate impact probe	Improve geodetic net; evaluate polar areas; study radiation environment
Payload (general)	AMIE, CIXS, SIR, plasma experiments	TC, MI, SP, relay satellites, X-ray, gamma-ray; altimeter; radar sounder, magnetometer, plasma imager	4-band micro-wave, IIM, X-ray, gamma-ray, energetic ions, stereo, altimeter	TMC, HySI, LLRI, HEX, Impact probe + C1XS, SARA, SIR2, miniSAR, M3, RADOM	LOLA, LROC, LAMP, LEND, CRaTER, Radiometer, LCROSS

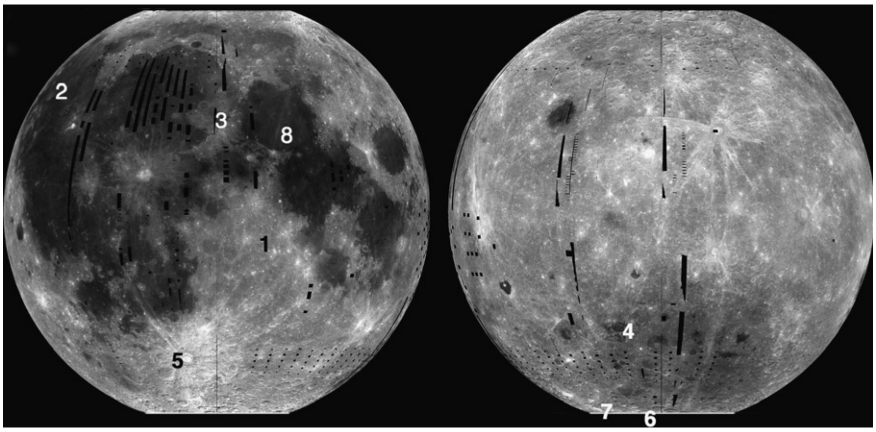

Fig. 1. Clementine albedo map of the Moon with the eight recommended ISCT areas indicated by number.

Table 2
Center coordinates of the eight L-ISCT sites

L-ISCT	Longitude (*E*)	Latitude (N+, S−)
1. Apollo 16 Highlands	15.5	−9.0
2. Lichtenberg rim	293.0	31.5
3. Apollo 15 (Hadley Rille)	3.7	26.1
4. SPA		
NW-N	175.5	−30.5
NW-S	165.0	−41.0
5. Tycho	348.8	−43.3
6. Polar shadows	118.0	−84.0
7. N. Schrödinger	135.0	−72.4
8. Mare Serenitatis (MS2)	21.4	18.7

as the series of serious lunar exploration missions are implemented.

2.1. Recommended coordination

Within the science plan of each individual mission, these eight target areas merit special study by the wide range of international sensors being flown to the Moon. Not all L-ISCT sites are ideal for all instrument calibration or validation applications. Due to different field of view or inherent measurement parameters, some L-ISCT sites are better suited for one type of measurement while other sites are better for others. Suggested categories of L-ISCT areas are presented for different instrument classes in Table 3. These categories are intended as guidelines for establishing a priority of L-ISCT measurements. A small number of targets are identified that are best suited to the specific instrument application, but the broader categories also allow cross-calibration of different classes of instruments among missions of the international community.

For mutual benefit, it is recommended that data for these targets be publicly released as soon as possible after measurement. L-ISCT data should first pass initial calibration by mission teams and then be released for coordinated validation among other teams. Cross validation is likely to be an iterative process, but when L-ISCT data from different instruments are in agreement, confidence in the measurements is high and all teams benefit. If data are not in agreement, possible sources of error can be sought and resolved. Teams of scientists are also encouraged to establish communication ties with similar teams on different missions to allow early comparisons (and improvement) of lunar data using these L-ISCT.

Table 3
Presented here are suggested categories of L-ISCT for different instrument classes – A: Best, most valuable; B: Good, quite useful; C: Supplemental

	1. Apollo 16	2. Lictenberg	3. Apollo 15	4. SPA-Th anomaly	5. Tycho	6. Polar shadows	7. North Schrodinger	8. Mare Serenitatis
Orbital imaging (⩽100 m/pixel)	A	B	A	B	B	A	A	C
UV–Vis–NIR spectroscopy	A	B	B	B	A	A	A	B
Altimetry & stereo	B	A	A	B	A	A	A	B
Thermal & radar imaging	A	B	B	B	A	A	A	C
Gamma-ray & neutron spectroscopy	A	B	C	A	B	A	B	A
X-ray spectroscopy	A	A	B	B	B	C	C	A
Particles, plasma, magnetometer	A	B	C	B	B	B	C	A
Micro-wave, sounder	B	A	B	A	B	B	A	A
Outreach	B	A	A	B	A	A	B	B

Since different instruments have inherently different calibration requirements, the optimal targets for cross-calibration will vary.

3. Recommended L-ISCT targets

3.1. L-ISCT #1 Apollo 16 Central Nearside Highlands

Target center: 9.0°S; 15.5°E

Principal rationale: This site is a large region of relatively uniform feldspathic highlands on the lunar nearside. Ground truth from Apollo samples provides excellent compositional calibration. Mature soil as well as several fresh craters of various sizes are found in the region.

An overview of the Apollo 16 region from a Clementine 750 nm albedo mosaic is shown in Fig. 2. The landing site is indicated with an arrow. An area of undisturbed (mature) soil that has been used for spectral calibrations is indicated by an "X". Clementine color composites of this area reveal the bright fresh craters to be relatively blue relative to surroundings (high 415/750 nm ratio).

The Apollo 16 mission was targeted to explore the central highlands of the Moon near Descartes Crater in order to assess the nature of the lunar highlands at considerable distance (~200 km) from any mare basalt deposits. The mission was originally intended to examine evidence for a possible volcanic origin of the Cayley plains as well as to examine unusual landforms in the vicinity of the landing site (hills, dome-like features) also proposed to be of possible volcanic origin (e.g., Ulrich et al., 1981). Apollo 16 Astronauts John Young and Charles Duke explored the landing region and found little to no evidence of volcanic activity at the site (Young et al., 1972). Instead, they quickly recognized that the rocks were composed of impact breccias, and that the intense crater and basin-scale bombardment history of the lunar highlands dominated the site. With the return and analysis of lunar samples, this region is now known to represent a large area of relatively uniform, but brecciated, feldspathic highlands on the nearside of the Moon.

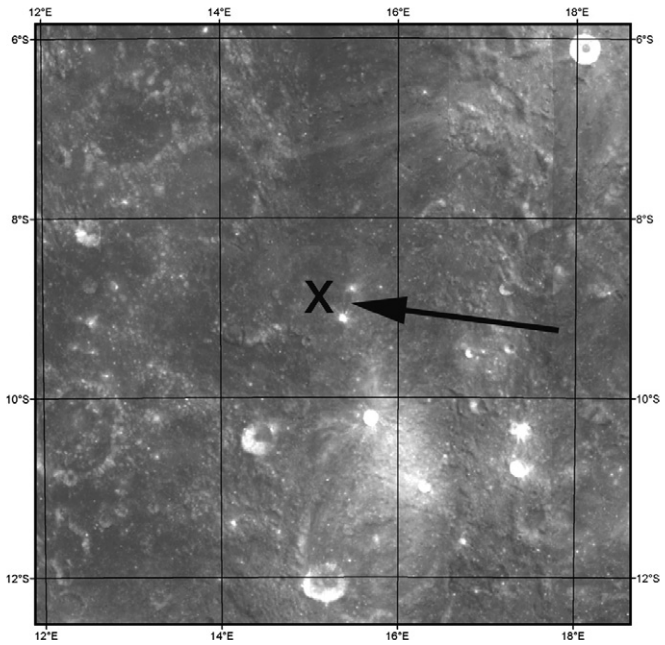

Fig. 2. Clementine 750 nm albedo data for the Apollo 16 region. The landing site area is indicated with an arrow. A large area of undisturbed (mature) soil that is often used for a calibration reference area is indicated with an X.

Apollo 16 has become an important site for the calibration of lunar spectroscopic data. Spectra of representative samples of well-developed soils collected at Apollo 16 and measured in Earth-based laboratories are used as "ground truth" for regions of undisturbed soil observed remotely (McCord et al., 1981; Pieters et al., 1994). The spectrum of a representative mature soil from this region, 62231, has been used extensively for spectral calibration of such areas of undisturbed highland soil such as that indicated with an "X" in Fig. 2. The spectrum of this Apollo 16 mature soil is shown in Fig. 3, and a more detailed discussion can be found in Pieters (1999). Digital spectroscopic data for 62231 can also be found at http://www.planetary.brown.edu/relabdocs/Apollo16_62231.html.

The Apollo 16 site is located in a central region that has been influenced by the ejecta deposits of many major impact basins (e.g., Nectaris, Imbrium, etc.; see Petro and Pieters, 2006) and a fundamental question is whether diverse datasets can be used to distinguish units formed by these basins and to separate these from local impact-generated units. The Apollo 16 area is an excellent test site for further calibration and for the deconvolution of complex highland stratigraphy (Stoffler et al., 1985). The presence of fresh craters of various sizes in this feldspathic region also provides contrasting material for studies of space-weathering and the influence of maturity on remote compositional analysis.

3.2. L-ISCT #2 Lichtenberg crater

Target center east rim: 31.5°N; 293°E

Principal rationale: Two very different types of basalt exist in the region, relatively old low-Ti and much younger high-Ti basalts. The young high-Ti basalts appear to over-

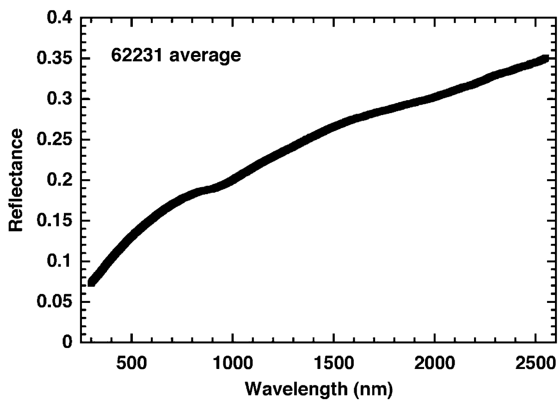

Fig. 3. Reflectance spectrum (reflectance factor) of Apollo 16 soil 62231. This spectrum of representative mature soil has often been used for "ground truth" calibration of remote spectral measurements. This laboratory spectrum was acquired with angle of incidence = 30° and emission angle = 0°. The spectrum is the average of several independent measurements.

lie fresh deposits from Lichtenberg crater. Age relations between basalt units and the crater Lichtenberg merit detailed assessment.

An overview of the Lichtenberg region using a Clementine 750 nm albedo mosaic is shown in Fig. 4. Lichtenberg crater is ~20 km in diameter. A SMART-1 image of the crater taken at a lower Sun angle is shown in Fig. 5. In the region surrounding Lichtenberg crater, basalt deposits appear to be superposed on the eastern ejecta deposit of this relatively young crater (Schultz, 1976; Hawke et al., 2000). Embayment relations between the young basalt and the crater ejecta are best seen in very low Sun-angle images (such as a few obtained from orbit during Apollo 15). Clementine color composite data and Lunar Prospector data both indicate that the young basalt to the east is Ti-rich and compositionally different from the older basalts to the north and west.

The characteristics and evolution of mare basalts record the nature of the lunar mantle and its melting as a function of time, and this provides essential constraints about the geological and thermal evolution of the Moon (e.g., Hiesinger and Head, 2006; Shearer et al., 2006). Analysis of the properties of surface units from remote sensing and returned samples provides abundant evidence for a wide range of basalt types and for changes in both the total flux of basaltic material produced and the composition of basaltic volcanism as a function of time (e.g., Hiesinger et al., 2000). Remote sensing data also identifies relatively young high-titanium basalts in the northwestern part of the nearside, an area not sampled by Apollo or Luna (e.g., Pieters, 1978; Hiesinger et al., 2003). Crater size-frequency distribution data have been interpreted to indicate that the basalts embaying Lichtenberg are actually among the youngest on the Moon, perhaps dating to the last billion years (e.g., Schultz and Spudis, 1983; Hiesinger et al., 2000, 2003).

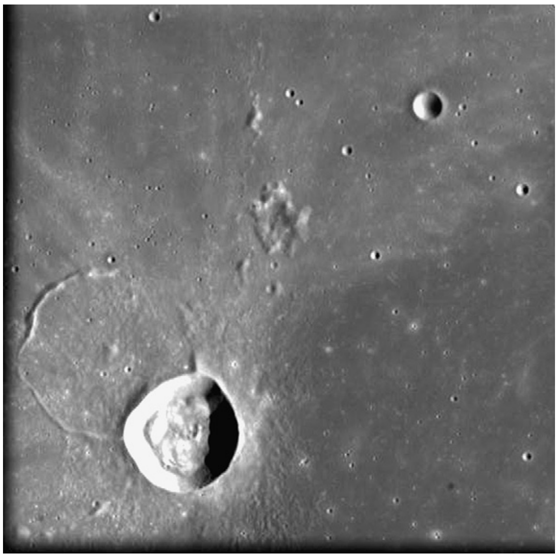

Fig. 5. SMART-1 image that includes the crater Lichtenberg under a different illumination. The AMIE camera obtained the images with a ground resolution of between approximately 186 and 195 m/pixel.

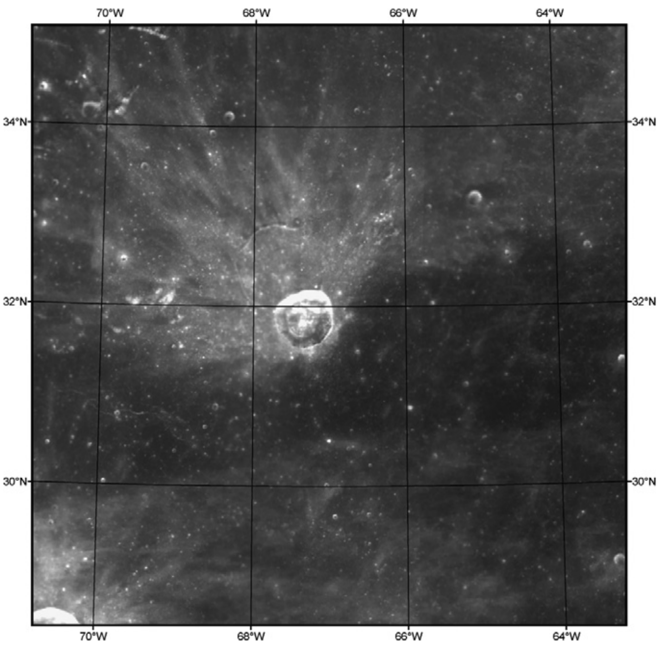

Fig. 4. Clementine 750 nm albedo image for the Lichtenberg region. Lichtenberg is ~20 km in diameter.

Important science goals for this region include the documentation of the geological relations between the young mare deposit and Lichtenberg crater ejecta, and a detailed comparison between the composition of these young high-titanium basalt and the much older high-titanium basalts found on the eastern part of the nearside (e.g., Mare Tranquillitatis). Do these young basalts represent a return to melting of a source region similar to that which formed the earlier deposits, or is there evidence for an entirely different petrogenetic process?

3.3. L-ISCT #3 Apollo 15 Hadley Rille

Target center: 26.1°N; 3.7°E

Principal rationale: The evolution of this site on a ring of Imbrium Basin records a diversity of fundamental geologic processes that are best addressed with diverse and integrated data. The wide range in scale, morphology, and composition of features at Hadley Rille make this target particularly challenging and interesting.

A Clementine high Sun albedo mosaic of the Apollo 15 region is shown in Fig. 6. A SMART-1 image of the area taken when the Sun is lower to the west is shown in Fig. 7. The rille can be seen crossing through the mare basalt in the center of the image. The Apennine Mountains form the eastern boundary and cross the image from upper right to lower left.

Hadley Rille, a sinuous depression over 130 km long, and the Apennine Mountains, the arcuate range of massifs forming part of the Imbrium Basin rim, have captured the interest of lunar scientists for decades. The Apollo 15 landing site was targeted to be on a mare region at the northern end of the Hadley Rille near the Apennine Mountains. The major goals were to assess the origin of the rille as well as the nature of the mountains and the thick section of lunar crustal material they might represent, and to determine the age of the lava plains and of the basin-forming event itself. Exploration of the region by Apollo 15 astronauts David Scott and James Irwin (Scott et al., 1972) identified several unusual and highly significant lunar samples and provided evidence for crater ejecta from Aristillus and Autolycus, two large craters further to the north in Imbrium Basin (Swann et al., 1972; Spudis and Ryder, 1986).

Samples from the site included two distinct types of mare basalts, as well as a suite of highland rocks, including anorthosites, Mg-suite plutonic rocks, impact melts, granulites, and breccias. Taken together with the results from other sites, the Apollo 15 data indicated that the Imbrium basin formed about 3.85 billion years ago and was resurfaced with maria at about 3.3 billion years ago. Also discovered at the Apollo 15 site was an aluminous non-mare basalt rich in KREEP and the pyroclastic green glass of ultramafic composition. Altogether, the Apollo 15 site is an exceptionally geologically complex and interesting region and new remote sensing data provides the opportunity to assess the provenance of many diverse materials as well as their modes of occurrence and abundance in the lunar crust.

Among questions of continued interest for the Hadley Rille area are: Is there evidence for stratigraphy and layering of basalts in the sinuous rille? To where did the lava that formed the rille eventually go in Mare Imbrium? Where are the Imbrium impact melt deposits? What is the distribution and source of the pyroclastic green glass?

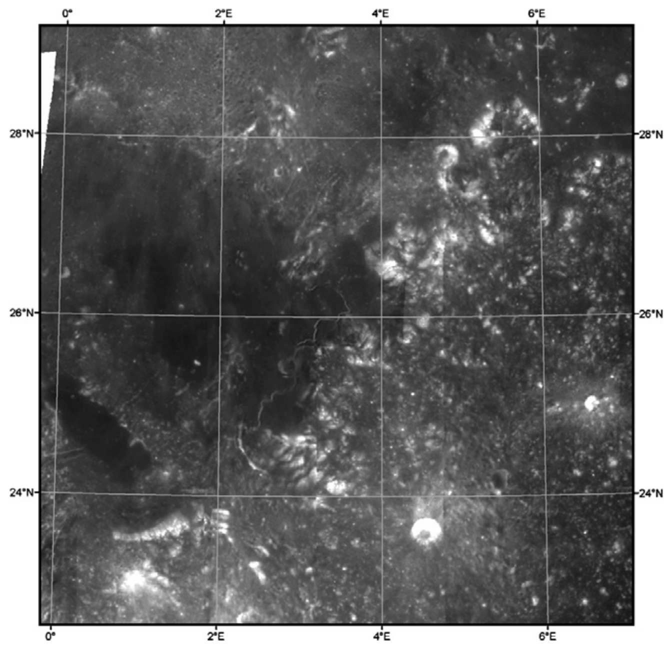

Fig. 6. Clementine 750 nm albedo image for the Apollo 15 region.

Fig. 7. SMART-1 image of the Apollo 15 area obtained by the AMIE camera.

Is there evidence for stratigraphy or sub-units in the basin ejecta deposits and can they be related to materials in the sample collection?

3.4. L-ISCT #4 South Pole-Aitken Basin Th-anomalies

Target center: 30.5°S, 175.5°E [northern target]; and 41°S, 165°E [southern target]

Principal rationale: A concentration of radiogenic elements observed in the NW region of South Pole-Aitken Basin may result from an asymmetry of excavated SPA lower crust/mantle or may be linked to antipode deposits from nearside basins. Several large-scale issues regarding the evolution of the lunar surface and interior are interwoven in this region.

Shown in Fig. 8 is an overview of key features of the 2500 km South Pole-Aitken Basin extracted from data collected by Clementine and Lunar Prospector. The basin's current designated "name" is derived from the fact that this enormous feature on the lunar farside extends from the South Pole to the crater Aitken, ~17° from the equator.

The South Pole-Aitken Basin is the largest, deepest, and oldest documented impact basin on the Moon (Wilhelms, 1987; Zuber et al., 1994). Clementine altimetry data indicate that the SPA Basin has a complex structure and a depth of more than 8 km. In spite of its tremendous size and depth (and in strong contrast to the smaller basins on the nearside), the SPA Basin has not been filled with mare basalt. Its interior thus likely contains materials derived from the impact event itself, which is expected to have excavated lower crust and/or possibly mantle materials. Lunar Prospector gamma-ray data (Lawrence et al., 2000, 2002, 2003) confirmed that the interior is geochemically distinct, with elevated iron and slightly elevated thorium content relative to the surrounding feldspathic highlands. Clementine albedo and color data independently reinforced the

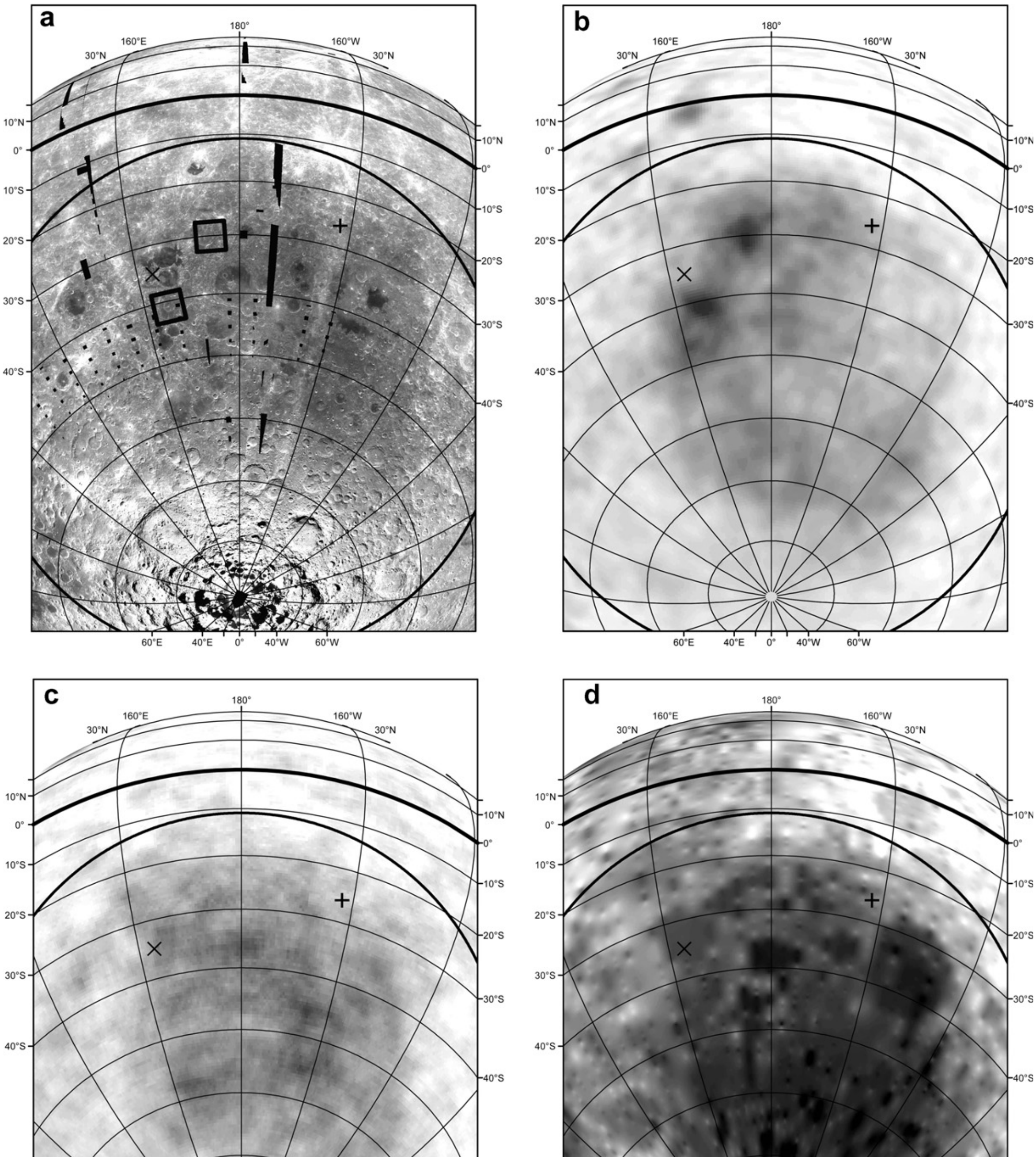

Fig. 8. Clementine and Lunar Prospector data for South Pole-Aitken Basin. The equator is the solid thick line at top. Latitude grid is in 10° increments; longitude grid is in 20° increments. "X" marks the nominal antipode of Imbrium and "+" the antipode of Serenitatis. (a) Clementine 750 nm albedo mosaic with L-ISCT areas indicated by black boxes; (b) LP Thorium; (c) LP Iron; [For (b) and (c) higher values are darker for clarity.] (d) Clementine Topography (low values are dark).

unusually mafic nature of the SPA interior (Lucey et al., 1995; Pieters et al., 2001).

Within the context of SPA's unique properties, a superimposed geochemical anomaly occurs in the northwest region of the basin (Fig. 8b). Two areas of notably higher thorium content are observed south of Ingenii and north of Leibnitz and are designated L-ISCT areas (Fig. 8a). They are found near the craters Oresme V (50 km diameter;

the southern L-ISCT) and Birkeland (82 km in diameter, the northern L-ISCT), but the locally elevated thorium may or may not be related to these impact features (Blewett et al., 2000; Garrick-Bethell and Zuber, 2005). If only one of these similar L-ISCT areas can be targeted by an instrument team, we suggest the northern target near the crater Birkeland.

Outstanding science questions include: What is the cause of the anomalous concentration of radiogenic elements in these areas? Could these local anomalies result from an asymmetry of lower crustal or upper mantle material excavated by SPA? Or could the material represent Th-rich ejecta converging at the antipode of the Imbrium or Serenitatis basin (Haskin, 1998; Wieczorek and Zuber, 2001)? How are these localized anomalies related the nature of the interior of this huge basin itself?

3.5. L-ISCT #5 Tycho crater

Target center: 43.3°S, 348.8°E

Principal rationale: Tycho is a large young crater on the nearside with an extensive ray system and a prominent dark halo of impact melt surrounding the crater. It is easily found with binoculars and sometimes can be seen by the naked eye during a full Moon.

Tycho crater, located in the south central portion of the nearside of the Moon is one of the most prominent features on the Moon as seen form Earth. A full Moon image of the southern nearside is shown in Fig. 9. Tycho exhibits a dark halo around its rim, produced by the emplacement of impact melt at the time of the crater's formation. Tycho's huge, bright ray system extends for thousands of km across the lunar surface. The rays are produced by ejecta that was excavated from the 84 km diameter crater and transported radially away from the crater, excavating, and mixing with local material when redeposited on the surface. Tycho is thought to have formed ~100 million years ago (Drozd et al., 1977). This age is derived from an exposure age date from the Apollo 17 site, where ejecta from Tycho (some 2000 km away) is thought to have modified the area around the landing site (Lucchita, 1977).

Shown in Fig. 10 is a Clementine 750 nm albedo image centered on Tycho and its surroundings. Tycho is characterized by a very fresh interior and rim deposit. The crater also has a prominent central peak and rough impact melt deposits covering the crater interior. In contrast to the surrounding feldspathic highlands, spectra from across the entire crater exhibit prominent mineral absorption bands due to the presence of high-Ca pyroxene (Pieters, 1993; Tompkins et al., 1999), suggesting that Tycho might have impacted into and excavated material from a lunar crustal pluton. Tycho is an excellent site for the study of fresh highland craters. Its prominence on the lunar nearside offers the opportunity for all viewers on Earth to connect to and recognize science targets on the Moon by observing the crater with the naked eye or with binoculars and small telescopes.

3.6. L-ISCT #6 Polar Region with shadows

Target center: 84°S, 118°E

Principal rationale: This area contains deep shadows and is located 6° from the South Pole. It is centered on the 28 km crater Idel'son L. This region does *not* exhibit high H abundance based on the Lunar Prospector results (Feldman et al., 2001; Lawrence et al., 2006) and thus provides neutron/gamma-ray background reference for H measurements at the pole. The area provides several calibration objectives for other instruments: light scattering (optical sensors), strong relief variations (altimetry, stereo), characterization of the interior of deeply shadowed areas (multiple sensors).

Fig. 9. Full Moon image of the crater Tycho showing its extensive ray system and dark halo.

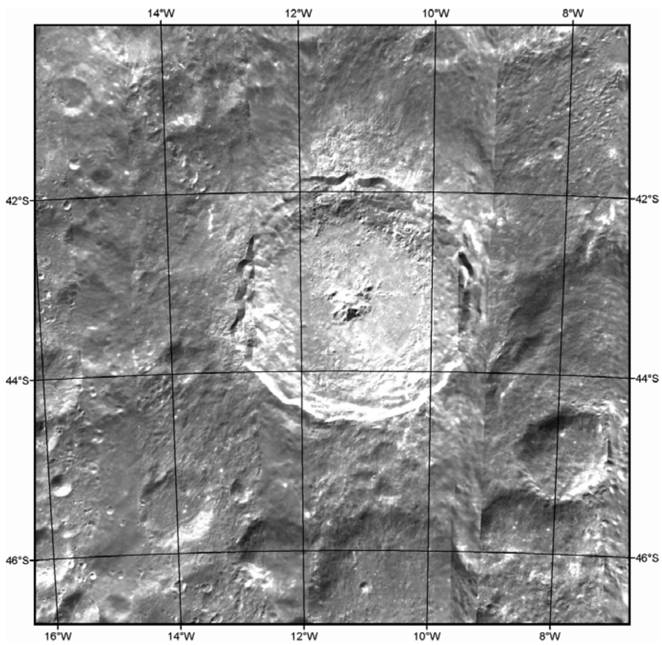

Fig. 10. Clementine 750 nm albedo image for the crater Tycho.

Fig. 11 contains the Polar Region Target #6 and is centered on the deeply shadowed crater Idel'son L.

3.7. L-ISCT #7 North Schrödinger

Target center: 72.4°S, 135°E

Principal rationale: Shrödinger Basin is located near the South Pole and is relatively well preserved; it is the second youngest basin on the Moon (Wilhelms, 1987). The target area includes a section of the north rim and interior mare fill. The high latitude allows this target to be frequently observed by the polar orbiting satellites (Table 1). The rough and smooth topography is well suited for repeated photometric and topography calibrations.

The northern rim of Shrödinger Basin (Target #7) is shown in Fig. 12, illustrating the range of morphology and topography present in this target region.

3.8. L-ISCT #8 Mare Serenitatis

Target center: 18.7°N, 21.4°E

Principal rationale: This area is centered on an optical standard in Mare Serenitatis used by many telescopic studies of the Moon, MS2 (e.g. McCord et al., 1972, 1981). The target area includes a large region of relatively uniform low-titanium mare basalt. To the south is a sharp boundary with an older high-titanium mare basalt of Mare Tranquillitatis. This boundary of two basalt types is prominent in both albedo and color (Mare Tranquillitatis being darker and "bluer"). Several small fresh craters occur within the region as do mare ridges and grabens.

Target #8 contains the southern edge of Mare Serenitatis and is shown in Fig. 13, which is centered on MS2.

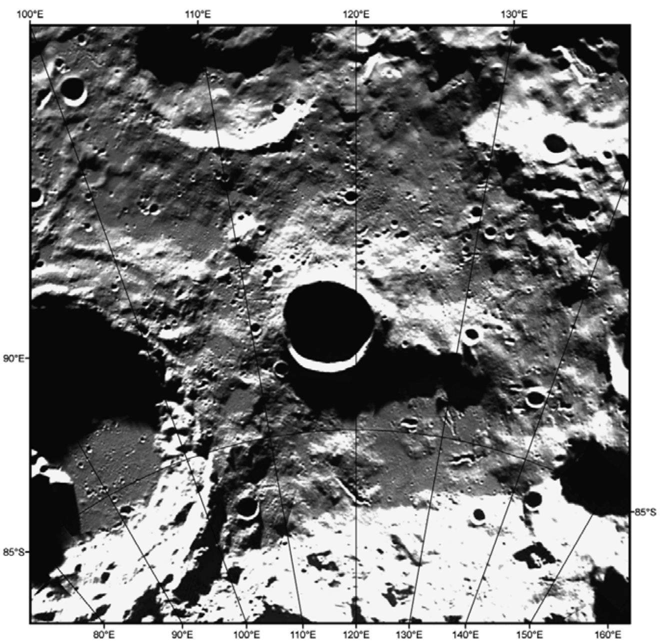

Fig. 11. Clementine 750 nm albedo image for an area 6° from the South Pole. The deeply shadowed 28 km crater in the center is Idel'son L.

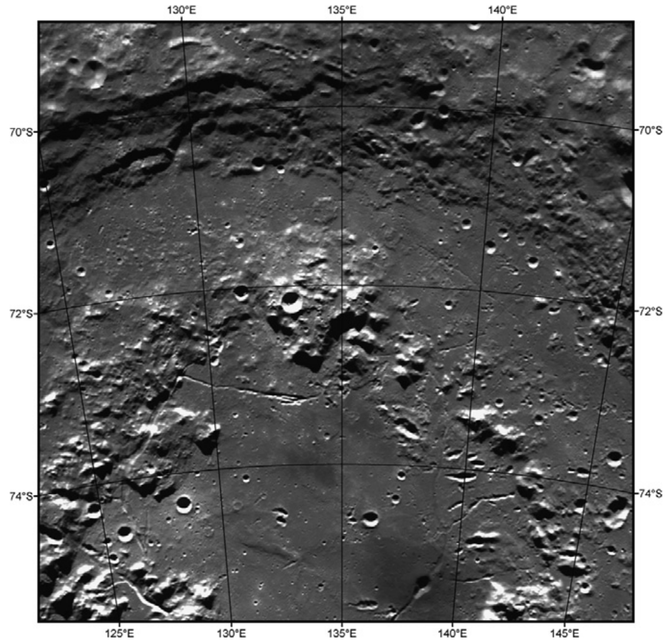

Fig. 12. Clementine 750 nm albedo image for an area at high latitudes containing the inner ring of the Schrödinger Basin as well as interior smooth plains (presumed to be basaltic).

4. Other coordination calibration issues

4.1. Time series measurements

Some data sets consist essentially of time series rather than observations of given locations, and hence require dif-

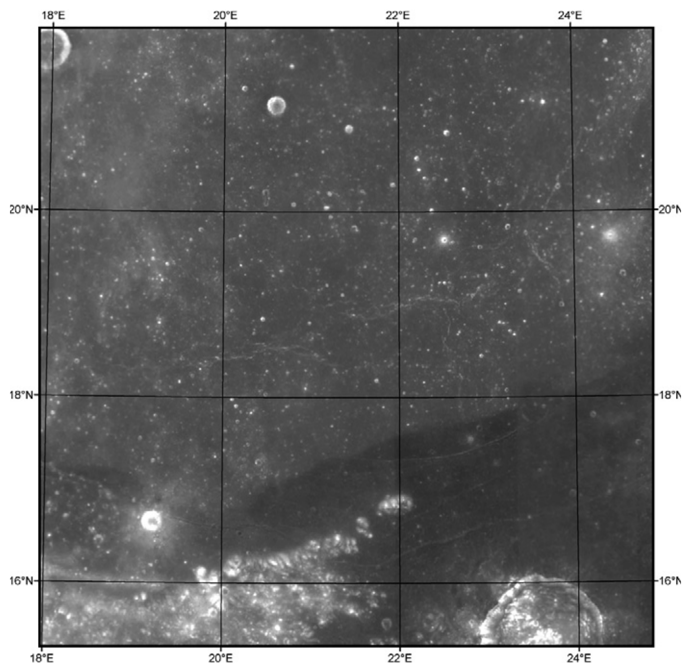

Fig. 13. Clementine 750 nm albedo image centered on an area in Mare Serenitatis frequently used as a calibration standard, MS-2. To the south the Serenitatis basalts are in sharp contact with the Ti-rich basalts of Mare Tranquillitatis.

ferent methodologies for cross-calibration. This can be particularly important for plasma instruments, where multipoint measurements greatly enhance the scientific productivity. Because the data are time series rather than maps, cross-calibration is in some senses less easy to plan with specific events. In general what is required is a stable and isotropic environment. Some regions or periods during mission operation may be more appropriate than others, such as long undisturbed intervals in the unperturbed Solar Wind. These can only be recognized as the information becomes available. However, it is very productive to identify the desired criteria beforehand and to establish communication links between participants that will allow implementation of coordination as the opportunity arises.

X-ray solar monitors, for example, represent a special case of this situation. X-ray fluorescence spectrometers rely on a well-measured input solar spectrum for quantitative elemental analyses. The lunar emission is particularly dependent on the intensity of solar illumination at energies immediately above (higher than) the fluorescence line. Because the activity of the Sun is highly variable, continuous monitoring of the solar X-ray spectrum is essential. Such solar monitor data may be readily shared between missions, provided that good cross-calibration of the monitors is achieved. Combining data from two spacecraft greatly reduces the unknowns in the continuous time series required. In this case, since in theory both instruments are observing simultaneously, the challenge is to ensure that the timings and pointing directions of the two instruments are well defined and understood.

4.2. Importance of repeat measurements and stability tests

Although all of the lunar missions have limitations in surface coverage and duration of mission operations and/or constraints on the amount of data that can be downlinked over a given period, there is significant value in measuring the same target more than once. This is particularly true for optical instruments. All near-future planned missions are in circular polar orbits (not Sun-synchronous), and the solar incident geometry of measurements for individual targets will thus vary each month. Since the target itself will not change over the timescale of an orbital mission, a time sequence of measurements at different geometries allows photometric models to be accurately tested. Similarly, a given solar illumination for a target will be similar twice a year and repeat measurements would allow the stability of instrument through-put to be monitored.

Because spacecraft resources are inevitably limited, we recommend the Apollo 16 target be the prime target for such repeat measurements. For narrow field of view instruments, this may require planning measurements using off-nadir pointing. However, since coverage is most limited for equatorial areas, we also recommend the high latitude North Schrödinger site as a secondary target for repeat calibration. The smooth terrain along the central part of this target area provides a good site for stability tests and will be more readily accessible for repeat measurements.

References

Blewett, D.T., Lucey, P.G., Hawke, B.R. et al. Compositional studies of the South Pole-Aitken Basin (Abstract, #1501). Lunar and Planetary Science XXXI, Houston, TX. 2000.

Chin, G., Brylow, S. Foote, M. et al. An Overview of the Lunar Reconnaissance Orbiter: Instrument Suite and Mission, paper presented at 8th ILEWG International Conference on Exploration and Utilization of the Moon, Beijing, China, 23–27 July, 2006.

Drozd, R.J., Hohenberg, M., Podosek, F.A., et al. Cosmic ray exposure story at Taurus-Littrow. Proc. Lunar Science Conf. 8, 3027–3043, 1977.

Feldman, W.C., Maurice, S., Lawrence, D.J., Little, R.C., Lawson, S.L., Gasnault, O., Wiens, R.C., Barraclough, B.L., Elphic, R.C., Prettyman, T.H., Steinberg, J.T., Binder, A.B. Evidence for water ice near the Lunar poles. J. Geophys. Res. 106, 23231–23252, 2001.

Föing, B.H., Frew, D., Almeida, M. et al. SMART-1 Mission Operations and Lunar Results, paper presented at 8th ILEWG International Conference on Exploration and Utilization of the Moon, Beijing, China, 23–27 July, 2006.

Garrick-Bethell, I., Zuber, M.T. An indigenous origin for the South Pole Aitken Basin thorium anomaly. Geophys. Res. Lett. 32, 13203, 2005.

Goswami, J.N., Thyagarajan, K., Annadurai, M. Chandrayaan-1 Mission: An Update, paper presented at 8th ILEWG International Conference on Exploration and Utilization of the Moon, Beijing, China, 23–27 July, 2006.

Hao, X.F., Zhou, J.S. The presently schedule and future development of the Chinese Chang'e Project, paper presented at 8th ILEWG International Conference on Exploration and Utilization of the Moon, Beijing, China, 23–27 July, 2006.

Haskin, L.A. The imbrium impact event and the thorium distribution at the lunar highlands surface. J. Geophys. Res. 103, 1679, 1998.

Hawke, B.R., Blewett, D.T., Lucey, P.G., et al. The origin of lunar crater rays. Icarus 170, 1–16, 2000.

Hiesinger, H., Head, J.W. New views of lunar geoscience: an introduction and overview, in: Jolliff, B., Wieczorek, M., Shearer, C., Neal, C. (Eds.), New Views of the Moon, Reviews in Mineraology and Geochemistry, vol. 60, pp. 1–81, 2006.

Hiesinger, H., Jaumann, R., Neukum, G., Head, J.W. Age of mare basalts on the lunar nearside. J. Geophys. Res. 105 (E12), 29239–29275, 2000.

Hiesinger, H., Head III, J.W., Wolf, U., Jaumann, R., Neukum, G. Ages and stratigraphy of mare basalts in Oceanus Procellarum, Mare Nubium, Mare Cognitum, and Mare Insularum, J. Geophys. Res. 108 (E7), 5065, doi:10.1029/2002JE001985, 2003.

Lawrence, D.J., Feldman, W.C., Barraclough, B.L., et al. Thorium abundances on the lunar surface. J. Geophys. Res. Planets 105 (E8), 20307–20331, 2000.

Lawrence, D.J., Feldman, W.C., Elphic, R.C., et al. Iron abundances on the lunar surface as measured by the Lunar Prospector gamma-ray and neutron spectrometers. J. Geophys. Res. 107 (E12), doi:10.1029/2001JE00153, 2002.

Lawrence, D.J., Elphic, R.C., Feldman, W.C., Prettyman, T.H., Gasnault, O., Maurice, S. Small-area thorium features on the lunar surface. J. Geophys. Res. 108 (E9), 5102, doi:10.1029/2003JE002050, 2003.

Lawrence, D.J., Feldman, W.C., Elphic, R.C., Hagerty, J.J., Maurice, S., McKinney, G.W., Prettyman, T.H. Improved modeling of Lunar Prospector neutron spectrometer data: implications for hydrogen deposits at the lunar poles. J. Geophys. Res. 111, E08001, doi:10.1029/2005JE002637, 2006.

Lucey, P.G., Taylor, G.J., Malaret, E. Abundance and distribution of iron on the Moon. Science 268, 1150–1153, 1995.

Lucchita, B.K. Crater clusters and light mantle at the Apollo 17 site – a result of secondary impact from Tycho. Icarus 30, 80–96, 1977.

McCord, T.B., Charette, M.P., Johnson, T.V., Lebofsky, L.A., Pieters, C.M., Adams, J.B. Lunar spectral types. J. Geophys. Res. 77, 1349–1359, 1972.

McCord, T.B., Clark, R.N., Hawke, B.R., McFadden, L.A., Owensby, P., Pieters, C.M., Adams, J.B. Moon: near-infrared spectral reflectance, a first good look. J. Geophys. Res. 86 (B11), 10883–10892, 1981.

Pieters, C.M. Mare basalt types on the front side of the Moon: a summary of spectral reflectance data. Lunar Planet. Sci. Conf. 9, 2825–2849, 1978.

Pieters, C.M. Compositional diversity and stratigraphy of the Lunar crust derived from reflectance spectroscopy, in: Remote Geochemical Analysis: Elemental and Mineralogical Composition, Cambridge University Press, pp. 309–339, 1993.

Pieters, C.M., Staid, M.I., Fischer, E.M., Tompkins, S., He, G. A sharper view of impact craters from Clementine data. Science 266, 1844–1848, 1994.

Pieters, C.M. The Moon as a spectral calibration standard enabled by lunar samples: the Clementine example. Workshop on New Views of the Moon II: Understanding the Moon Through the Integration of Diverse Datasets (Abstract, #8025), Houston, TX, LPI, 1999.

Pieters, C.M., Head, J.W., Gaddis, L., Jolliff, B., Duke, M. Rock types of South Pole-Aitken basin and extent of basaltic volcanism. J. Geophys. Res. 106 (E11), 28001–28022, 2001.

Petro, N.E., Pieters, C.M. Modeling the provenance of the Apollo 16 regolith. J. Geophys. Res. 111, E09005, doi:10.1029/2005JE002559, 2006.

Schultz, P.H. Moon Morphology. University of Austin Press, Austin, TX, 626 pp, 1976.

Schultz, P.H., Spudis, P.D. Beginning and end of lunar mare volcanism. Nature, 233–236, 1983.

Shearer, C.K., Hess, P.C., Wieczorek, M.A., et al. Thermal and magmatic evolution of the Moon, in: Jolliff, B., Wieczorek, M., Shearer, C., Neal, C. (Eds.), New Views of the Moon, Reviews in Mineraology and Geochemistry, vol. 60, pp. 365–518, 2006.

Scott, D.R., Worden, A.M., Irwin, J.B. Crew Observations, in: Apollo 15 Preliminary Science Report, NASA SP-289, pp. 4–1 to 4–4, 1972.

Spudis, P.D., Ryder, G. (Eds.), Workshop on the Geology and Petrology of the Apollo 15 Landing Site, LPI Technical Report 86-03, Lunar and Planetary Institute, Houston, 126 pp. 1986.

Stoffler, D., Bischoff, A., Borchardt, R., et al. Composition and evolution of the lunar crust in the Descartes Highlands, Apollo 16. Proc. Lunar Planet. Sci. Conf. 15th, J. Geophys. Res. 89, C449–C506, 1985.

Swann, G.A., Bailey, N.G., Batson, R.M., et al. Preliminary geologic investigations of the Apollo 15 landing site, in: Apollo 15 Preliminary Science Report, NASA SP-289, pp. 4–1 to 4–4, 1972.

Takizawa, Y., Sasaki, S., Kato, M., Takahashi, M. SELENE Project Status, paper presented at 8th ILEWG International Conference on Exploration and Utilization of the Moon, Beijing, China, 23–27 July, 2006.

Tompkins, S., Hawke, B.R., Pieters, C.M. Distribution of materials within the crater Tycho: evidence for large gabbroic bodies in the highlands (Abstract #1573) Lunar and Planetary Science XXX, 1999.

Ulrich, G.E., Hodges, C.A., Muehlberger, W.R. (Eds.), Geology of the Apollo 16 Area, Central Lunar Highlands, USGS Prof. Paper 1048, 539 pp., 1981.

Wieczorek, M.A., Zuber, M.T. A Serenitatis origin for the Imbrian grooves and South Pole-Aitken thorium anomaly. J. Geophys. Res. 106, 27853–27864, 2001.

Wilhelms, D.E. The Geologic History of the Moon, U.S. Geological Survey Prof. Paper 1348, 302pp, 1987.

Young, J.A., Mattingly, K.A., Duke, C.M. Crew Observations, in Apollo 16 Preliminary Science Report, NASA SP-315, pp. 5–1 to 5–6, 1972.

Zuber, M.T., Smith, D.E., Lemoine, F.G., Neumann, G.A. The shape and internal structure of the Moon from the Clementine mission. Science 266, 1839–1843, 1994.